

PAPER



Cite this: *Soft Matter*, 2018,
14, 4702

Received 29th March 2018,
Accepted 18th May 2018

DOI: 10.1039/c8sm00662h

rsc.li/soft-matter-journal

Interactions between amphoteric surfaces with strongly overlapping double layers

Mark Vis,^{id}*^a Remco Tuinier,^{id}^{ab} Bonny W. M. Kuipers,^{id}^b Agienus Vrij^b and Albert P. Philipse^{id}^b

The entropic repulsion between strongly overlapping electrical double-layers from two parallel amphoteric plates is described *via* the Donnan equilibrium in the limit of zero electric field. The plates feature charge-regulation and the inter-plate solution is in equilibrium with a reservoir of a monovalent electrolyte solution. A finite electric potential and disjoining pressure is found at contact between the plates, due to a complete discharging of the plates. For low potentials, the decay of potential and pressure is fully governed by a characteristic length scale and the contact potential. Additionally, for large separations we find a universal inverse square decay of disjoining pressure, irrespective of the contact potential. The results of the Donnan theory show quantitative agreement with self-consistent field computations that solve the full Poisson equation.

1 Introduction

When two charged surfaces immersed in an electrolyte solution move sufficiently far apart such that mid-plane electrical potentials are small, double-layer repulsions between the surfaces can be evaluated from the Debye–Hückel solution of the linearized Poisson–Boltzmann (PB) equation.^{1–10} Upon approach of the two plates, mid-plane potentials increase such that the approximation of weak double-layer overlap breaks down.

It has been pointed out^{11–14} that when two identical charged surfaces come sufficiently near, another simplifying limit is approached: for inter-plate distances below the Debye length, the electric field between the surfaces gradually vanishes throughout. Then a regime is entered where ions diffuse in a spatially constant electrical potential (in contrast, for larger separations, the electric field is only zero at the mid-plane between the plates). For the case of ideal ions, the calculation of this spatially constant potential, also known as the Donnan potential, is straightforward. It leads—without any further assumptions—to analytical expressions for the disjoining pressure, *i.e.*, the external pressure that is needed to fix the repulsive plates at a certain distance.¹³ It should be stressed that this inverse square decay differs in origin from the inverse-square decay that is observed in the salt-free, counterion-only limit.^{12,15}

These Donnan disjoining pressures agree quite well with numerical solutions of the PB equation up to inter-plate distances as large as about the Debye length,¹³ in marked contrast to the exponential decay that results from the weak-potential Debye–Hückel approximation. Furthermore, recently it was shown by Landman *et al.* that the algebraic Donnan disjoining pressure could explain peculiar scaling of interbilayer separation with concentration in structures of self-assembled microtubes.¹⁶ Their observations represent, as far as we know, the first experimental support for the zero-field Donnan model. The Donnan model, it should be noted, was also employed by Per Linse and co-workers in their profound computational study of polyelectrolyte gels in equilibrium with a salt reservoir solution.^{17,18}

The zero-field Donnan treatment¹³ for constant-charge plates, was recently extended¹⁴ to surfaces with a regulated charge density. There, surface charge was due to a single association–dissociation equilibrium, which excludes the possibility of a net-charge sign reversal induced by a pH change: in other words, those surfaces had no iso-electric point (IEP).¹⁴ Surfaces of common inorganic colloids, composed of materials such as silica, aluminium (hydr)oxides and iron (hydr)oxides, of course do have an IEP owing to pH-dependent protonation and deprotonation of surface hydroxyl groups. The aim of the present work is therefore to generalize the Donnan treatment¹⁴ to amphoteric surfaces, *i.e.*, surfaces grafted with a single type of molecules that can accept as well as release cations, yielding positive or negative charge densities depending on pH.

This paper is structured as follows. Derivations of electrical potentials, dissociation degrees, and disjoining pressures for amphoteric surfaces *via* Donnan zero-field theory are given in

^a Laboratory of Physical Chemistry, Faculty of Chemical Engineering and Chemistry & Institute for Complex Molecular Systems, Eindhoven University of Technology, The Netherlands. E-mail: M.Vis@tue.nl

^b Van 't Hoff Laboratory for Physical and Colloid Chemistry, Debye Institute for Nanomaterials Science, Utrecht University, The Netherlands

Section 2. Self-consistent field (SCF) computations, detailed in Section 3, are done to assess the validity of the zero-field calculations done for ideal ions. The SCF lattice computations, which solve the full PB equation for ions and solvent molecules of finite size, are compared in Section 4 to predictions from Donnan theory. The paper is finalized with general conclusions in Section 5.

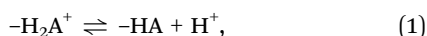
2 Zero-field Donnan theory

In this section we will describe the repulsion between two amphoteric, charge regulated surfaces using zero-field Donnan theory. We will first give a description of the system at hand, followed by derivations of the Donnan potential, degree of dissociation, and disjoining pressure, with a focus on the limiting behavior at low potentials.

2.1 General description of the system

Consider two parallel surfaces separated by a distance h , immersed in an electrolyte solution. The electrolyte is a simple strong monovalent acid such as HCl or HNO₃. The inter-plate region is in equilibrium with a reservoir of constant salt concentration ρ_s , as sketched in Fig. 1.

The surface contains amphoteric groups $-AH$, that can both accept and release ions. The following equilibria are accounted for:



with the following equilibrium constants:

$$K_1 = \frac{\sigma_{HA}\rho_+}{\sigma_{H_2A^+}}, \quad (3)$$

$$K_2 = \frac{\sigma_{A^-}\rho_+}{\sigma_{HA}}. \quad (4)$$

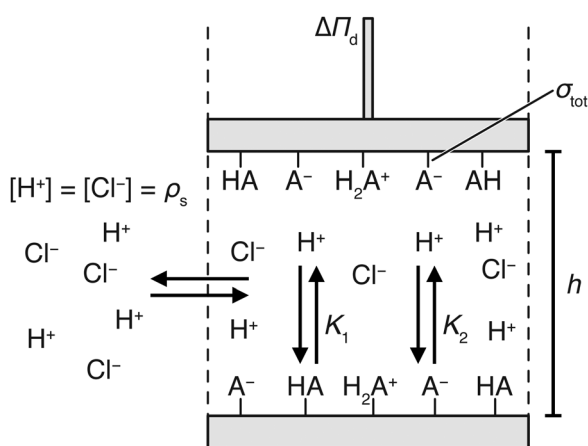
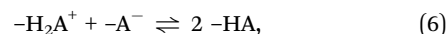


Fig. 1 Schematic overview of the system under consideration. Two plates, grafted with amphoteric groups ($-AH$), are in equilibrium with a salt reservoir containing a simple strong acid (HCl) at fixed concentration ρ_s . The amphoteric groups, with density σ_{tot} , can acquire or release protons with equilibrium constants K_1 and K_2 respectively, such that the surfaces become positively or negatively charged. An external pressure $\Delta \Pi_d$ is required to fix the distance h between the plates.

Here ρ_+ denotes the number density of cations, in this case H^+ , at the surface of the plates. The surface densities are denoted by σ_i ; the total surface density of the amphoteric groups is given by

$$\sigma_{tot} = \sigma_{H_2A^+} + \sigma_{HA} + \sigma_{A^-} \quad (5)$$

and is assumed to be constant. It should be mentioned that, through eqn (1) and (2), we implicitly also incorporate the following surface equilibrium



with equilibrium constant

$$K_3 = \frac{\sigma_{HA}^2}{\sigma_{H_2A^+}\sigma_{A^-}} = \frac{K_1}{K_2}. \quad (7)$$

We will follow the convention of referring to the numerical values of the equilibrium constants through their pK 's, defined as $pK_i \equiv -\log K_i$.

From now on, we consider the limit of strongly overlapping electric double layers, *i.e.*, it is assumed that all inter-plate separations are smaller than approximately the Debye length, defined as

$$\lambda_D \equiv \frac{1}{\sqrt{8\pi\lambda_B I}}, \quad (8)$$

where $\lambda_B \equiv e^2/(4\pi\epsilon_0\epsilon_r k_B T)$ is the Bjerrum length of the medium (with e the elementary charge, ϵ_0 the vacuum permittivity, ϵ_r the relative permittivity, k_B the Boltzmann constant, and T the absolute temperature) and I is the ionic strength. Under these conditions, the electric field between the plates is negligible and the ions are distributed homogeneously: ρ_+ is a spatial constant.

By solving eqn (1), (2) and (5) for σ_{A^-} and $\sigma_{H_2A^+}$ simultaneously, we find that the degree of dissociation into positively and negatively charged sites is given by

$$\alpha_+ \equiv \frac{\sigma_{H_2A^+}}{\sigma_{tot}} \quad (9)$$

$$= \frac{\left(\frac{\rho_+}{\rho_s}\right)^2}{\left(\frac{\rho_+}{\rho_s}\right)^2 + k_1 \frac{\rho_+}{\rho_s} + k_1 k_2}, \quad (10)$$

and

$$\alpha_- \equiv \frac{\sigma_{A^-}}{\sigma_{tot}} \quad (11)$$

$$= \frac{k_1 k_2}{\left(\frac{\rho_+}{\rho_s}\right)^2 + k_1 \frac{\rho_+}{\rho_s} + k_1 k_2}, \quad (12)$$

where the dimensionless equilibrium constants k_1 and k_2 , defined through

$$k_i \equiv K_i/\rho_s, \quad (13)$$

have been introduced.

When the plates are infinitely far apart, the concentration of ions in the inter-plate region becomes equal to that of the reservoir. Hence we find for the maximum degree of dissociation:

$$\alpha_+^{\max} = \frac{1}{1 + k_1 + k_1 k_2}, \quad (14)$$

$$\alpha_-^{\max} = \frac{k_1 k_2}{1 + k_1 + k_1 k_2}. \quad (15)$$

For comparison with SCF computations, it is convenient to vary the pH of systems while keeping the Debye length λ_D constant through addition of inert background salt. This scenario can be described by choosing effective values for pH, pK_1 , and pK_2 . For instance, SCF computations at $I = 10^{-6}$ M, pH = 6.5, $pK_1 = 1$, and $pK_2 = 13$ may be mapped onto a system with pH = 6.0, $pK_1 = 0.5$, and $pK_2 = 12.5$.

2.2 Donnan potential

The concentration of cations and anions in the inter-plate region is assumed to be linked to the salt concentration in the reservoir through a Boltzmann distribution,

$$\rho_{\pm} = \rho_s \exp(\mp u), \quad (16)$$

where $u = e\psi/(k_B T)$ is the dimensionless Donnan potential difference of the inter-plate region w.r.t. the reservoir, with ψ the potential difference. It is emphasized that u is assumed to be a spatial constant in our zero-field Donnan model. It should be compared to the mid-plane potential resulting from more elaborate approaches (such as the full Poisson–Boltzmann theory incorporated in our SCF computations), because halfway between the two plates the local electric field is zero.

An expression for the potential u may be derived based on the boundary condition that the inter-plate region is electrically neutral. Electroneutrality entails that

$$\rho_+ h + 2\sigma_{\text{tot}}\alpha_+ = \rho_- h + 2\sigma_{\text{tot}}\alpha_-, \quad (17)$$

which can be rewritten as

$$\sinh u = \frac{\sigma_{\text{tot}}}{\rho_s h} (\alpha_+ - \alpha_-), \quad (18)$$

using eqn (10), (12) and (16) and $(\rho_+ - \rho_-)/(2\rho_s) = -\sinh u$. It turns out that it is convenient to rewrite this as

$$\sinh u = \frac{\lambda}{h} \frac{\alpha_+ - \alpha_-}{\alpha_+^{\max} - \alpha_-^{\max}} \quad (19a)$$

$$= \frac{\lambda}{h} \frac{1 + k_1 + k_1 k_2}{1 - k_1 k_2} \frac{\exp(-2u) - k_1 k_2}{\exp(-2u) + k_1 \exp(-u) + k_1 k_2}, \quad (19b)$$

where

$$\lambda \equiv \frac{\sigma_{\text{tot}}}{\rho_s} (\alpha_+^{\max} - \alpha_-^{\max}) \quad (20a)$$

$$= \frac{\sigma_{\text{tot}}}{\rho_s} \frac{1 - k_1 k_2}{1 + k_1 + k_1 k_2}. \quad (20b)$$

The parameter λ has the unit of length and its absolute magnitude sets the characteristic length scale for repulsions

between strongly overlapping double layers. Note that the sign of λ in this definition follows the sign of the surface charge: it is positive for a net cationic surface and negative for a net anionic surface, because $k_1 k_2 < 1$ for the former and $k_1 k_2 > 1$ for the latter.

The length scale λ can be related to the Gouy–Chapman length,¹² which is inversely proportional to the number of charges σ per unit area of a surface:

$$\lambda_{\text{GC}} \equiv (2\pi\lambda_B|\sigma|)^{-1}. \quad (21)$$

In our case, σ (and consequently λ_{GC}) continuously varies with separation distance between the plates, but as a reference we may take the Gouy–Chapman length at infinite separation:

$$\lambda_{\text{GC}}^{\max} \equiv (2\pi\lambda_B\sigma_{\text{tot}}|\alpha_+^{\max} - \alpha_-^{\max}|)^{-1}, \quad (22)$$

from which λ follows as

$$|\lambda| = 4\lambda_D^2/\lambda_{\text{GC}}^{\max}. \quad (23)$$

Eqn (19) has a rather involved (though analytic) solution since it is cubic in $\exp u$ and, for brevity, we do not show it here. A straightforward solution for the Donnan potential at contact is available however. It follows from the fact that, for $h \rightarrow 0$, the last fraction in eqn (19b) must become zero:

$$\frac{\exp(-2u) - k_1 k_2}{\exp(-2u) + k_1 \exp(-u) + k_1 k_2} = 0 \quad \text{for } h \rightarrow 0. \quad (24)$$

Therefore, the contact electric potential u_0 is given by

$$u_0 = -\ln \sqrt{k_1 k_2} \quad (25)$$

which is valid for potentials of arbitrary magnitude. This result entails that the contact potentials for amphoteric surfaces remain finite, whereas for surfaces with a single dissociation equilibrium ($k_1 \rightarrow \infty$ or $k_2 \rightarrow 0$) or with a fixed charge ($k_1 \rightarrow \infty$ and $k_2 \rightarrow 0$) the contact electric potential diverges.^{13,14,19} It should also be noted that the contact potential is independent of the surface density σ_{tot} of the amphoteric groups.

In the limit of small potentials, more straightforward limiting solutions can be obtained. When retaining only the first order terms of eqn (19), it can be shown that

$$u \simeq \left(\frac{1}{u_0^{\text{eff}}} + \frac{h}{\lambda} \right)^{-1} \quad \text{for } |u| \ll 1, \quad (26)$$

where we denote u_0^{eff} as the effective Donnan potential at contact ($h = 0$) in the low-potential limit, defined as

$$u_0^{\text{eff}} \equiv -\frac{(1 - k_1 k_2)(1 + k_1 + k_1 k_2)}{k_1(1 + 4k_2 + k_1 k_2)}. \quad (27)$$

It is noted that u_0 and u_0^{eff} have the same value for small contact potentials. This does not hold for large contact potentials (e.g., far from the IEP), however the definition of eqn (27) ensures that whenever the Donnan potential u becomes small upon increasing separation, eqn (26) will still predict the correct Donnan potential, even if u_0 and/or u_0^{eff} are large. This would not be the case if one would naively use u_0 (eqn (25)) in place of u_0^{eff} in eqn (26). This is the reason that eqn (27) can be viewed as an effective or apparent contact potential that one would probe at intermediate separations.

From eqn (26) it is evident that the decay of the Donnan potential with increasing separation h is fully set by the effective contact potential u_0^{eff} and length scale λ alone. We can make a series expansion of eqn (26) for small inter-plate separations h to find that

$$u \simeq u_0^{\text{eff}} \left[1 - u_0^{\text{eff}} \frac{h}{\lambda} + \left(u_0^{\text{eff}} \frac{h}{\lambda} \right)^2 + \dots \right] \quad (28)$$

$$\simeq u_0^{\text{eff}} \left(1 - u_0^{\text{eff}} \frac{h}{\lambda} \right) \quad \text{for } |u| \ll 1 \text{ and } h \rightarrow 0, \quad (29)$$

whereas for large separations,

$$u \simeq \frac{\lambda}{h} \left[1 - \frac{1}{u_0^{\text{eff}}} \frac{\lambda}{h} + \left(\frac{1}{u_0^{\text{eff}}} \frac{\lambda}{h} \right)^2 + \dots \right] \quad (30)$$

$$\simeq \frac{\lambda}{h} \quad \text{for } |u| \ll 1 \text{ and } h \rightarrow \infty. \quad (31)$$

Interestingly, the Donnan potential at large separations is independent of u_0^{eff} to leading order. In other words, for sufficiently large separations, the decay of $u(h)$ shows universal behavior, when the separations are normalized to the length scale λ .

2.3 Degree of dissociation

The degree of dissociation can be obtained from substitution of eqn (16) into eqn (10) and (12):

$$\alpha_+ = \frac{\exp(-2u)}{\exp(-2u) + k_1 \exp(-u) + k_1 k_2}, \quad (32)$$

$$\alpha_- = \frac{k_1 k_2}{\exp(-2u) + k_1 \exp(-u) + k_1 k_2}. \quad (33)$$

The net degree of dissociation, which is proportional to the charge density of the surfaces, is therefore given by

$$\alpha_+ - \alpha_- = \frac{\exp(-2u) - k_1 k_2}{\exp(-2u) + k_1 \exp(-u) + k_1 k_2}. \quad (34)$$

For two plates at contact, using eqn (25), it follows that

$$\alpha_+(h=0) = \alpha_-(h=0) = \frac{1}{2 + \sqrt{\frac{k_1}{k_2}}}. \quad (35)$$

Since the net charge density on each plate is proportional to $\alpha_+ - \alpha_-$, this means that two amphoteric plates at contact fully discharge each other. This full net discharge of the plates at contact in turn enables the finite contact potential u_0 .

For low potentials, eqn (32) and (33) may be linearized to yield

$$\alpha_+ \simeq \frac{1 - 2u}{(1 - 2u) + k_1(1 - u) + k_1 k_2} \quad (36)$$

$$= \frac{\alpha_+^{\text{max}} \left[1 - 2u_0^{\text{eff}} \left(1 + u_0^{\text{eff}} \frac{h}{\lambda} \right)^{-1} \right]}{1 - \alpha_+^{\text{max}} u_0^{\text{eff}} (2 + k_1) \left(1 + u_0^{\text{eff}} \frac{h}{\lambda} \right)^{-1}} \quad \text{for } |u| \ll 1, \quad (37)$$

and

$$\alpha_- \simeq \frac{k_1 k_2}{(1 - 2u) + k_1(1 - u) + k_1 k_2} \quad (38)$$

$$= \frac{\alpha_-^{\text{max}} k_1 k_2}{k_1 k_2 - \alpha_-^{\text{max}} u_0^{\text{eff}} (2 + k_1) \left(1 + u_0^{\text{eff}} \frac{h}{\lambda} \right)^{-1}} \quad \text{for } |u| \ll 1, \quad (39)$$

where eqn (26) was employed. Likewise, the corresponding limits of small and large separations may be obtained using eqn (29) and (31), but for brevity we omit them here.

2.4 Disjoining pressure

The expressions for u also allow to calculate the disjoining pressure of the charge-regulated plates. The disjoining pressure, scaled to the osmotic pressure of the salt reservoir, is defined as

$$\Delta \tilde{\Pi} \equiv \frac{\Delta \Pi}{2\rho_s k_B T} \quad (40)$$

$$= \frac{\rho_+ + \rho_- - 2\rho_s}{2\rho_s}. \quad (41)$$

Inserting the Boltzmann distribution of eqn (16) yields

$$\Delta \tilde{\Pi} = \cosh u - 1. \quad (42)$$

Eqn (42) is also valid when there is only weak overlap of the double layers, as long as the electric field in the mid-plane is zero and the ions in the mid-plane behave ideally.

For small potentials, $\cosh u - 1 \simeq \frac{1}{2}u^2$. Using eqn (26), (29) and (31), we find:

$$\Delta \tilde{\Pi} \simeq \frac{1}{2} \left(\frac{1}{u_0^{\text{eff}}} + \frac{h}{\lambda} \right)^{-2} \quad \text{for } |u| \ll 1, \quad (43)$$

$$\Delta \tilde{\Pi} \simeq \frac{1}{2} \left(u_0^{\text{eff}} \right)^2 \left(1 - 2u_0^{\text{eff}} \frac{h}{\lambda} \right) \quad \text{for } |u| \ll 1 \text{ and } h \rightarrow 0, \quad (44)$$

$$\Delta \tilde{\Pi} \simeq \frac{1}{2} \left(\frac{\lambda}{h} \right)^2 \quad \text{for } |u| \ll 1 \text{ and } h \rightarrow \infty. \quad (45)$$

It follows that the inverse square decay, first predicted for constant-charge surfaces¹³ and charge-regulated surfaces with a single equilibrium,¹⁴ also holds for amphoteric surfaces, as long as $u_0^{\text{eff}} \frac{h}{\lambda} \gg 1$. The prefactor u_0^{eff} in this limit entails, perhaps somewhat counter-intuitively, that for small contact potentials, large separations are necessary to achieve this condition. For constant-charge and single-equilibrium surfaces, the contact potential is infinite, thus this subtlety is not present for those surfaces. For infinite contact potentials, eqn (43) directly reduces to eqn (45).

3 SCF computations

In order to assess the validity of our theoretical approximations in the previous section, we performed self-consistent field (SCF) calculations to compute the thermodynamic properties of

two infinite parallel amphoteric plates in an electrolyte solution. In contrast to the zero-field approximation, the SCF computations solve the full Poisson equation (on a mean-field level) and assume a finite size for ions and solvent. SCF theory has been extensively discussed in the literature before, see ref. 20–27 for details. Here we will mostly focus on a description of the parameters used in the computations.

We perform our calculations on the basis of the numerical lattice approximation of Scheutjens and Fler.^{20,23} In the Scheutjens–Fler method, space is represented by a set of lattice sites. For the application of SCF theory in this work, the focus is on a flat geometry in which T lattice layers are considered. The lattice layers are numbered $z = 0, 1, 2, \dots, T, T + 1$, where the first plate is located at $z = 0$ and the second plate at $z = T + 1$. The inter-plate distance is given by $h = bT$, where b is the size of a lattice site. The solution between these plates is in equilibrium with a reservoir of constant chemical potential.

Our calculations are performed with the following parameters. The size of a lattice site is set to $b = 0.3$ nm and all ions, solvent molecules, and surface groups in the system occupy a single lattice site. We assume ideal behavior, so all Flory–Huggins interaction parameters χ are set to zero.^{26,28} The relative permittivity of all components is fixed to 80 to model water and the temperature $T = 298.15$ K. The self-dissociation of water is modeled with an equilibrium constant $pK_w = 14$, leading to a minimum ionic strength $I = 10^{-7}$ M at a pH of 7 and higher values at different pH. Additional (inert) background salt is added in certain calculations; the reported ionic strength is the total in the reservoir due to inert background salt and the acid–base equilibrium at given pH. The two plates are grafted with weakly acidic sites located directly next to the plates, *i.e.*, at $z = 1$ and $z = T$, with a density σ_{tot} on each plate. The minimum number of lattice layers between the plates is therefore $T = 2$, *i.e.*, such that the grafted groups touch but do not interpenetrate.

Two primary outcomes of the SCF computations that are relevant for comparison to our zero-field theory are the electrostatic potential profiles $\psi(z)$ and volume fraction profiles $\phi(z)$ of all components. The electrostatic zero-field potential from the Donnan theory is compared to the potential at the mid-plane ($\psi(T/2)$) of the SCF computations. The degrees of dissociation α_+ and α_- follow from the fraction of surface groups that are in a positive or negative state, respectively.

The disjoining pressure can be obtained in various ways, for instance from the derivative of the semi-open grand potential with inter-plate separation.¹⁴ Here, we opt to obtain the disjoining pressure from the density of the ions in the mid-plane ($z = T/2$). Since at the mid-plane the electric field is exactly zero and all interaction parameters are set to zero, the dimensionless disjoining pressure follows analogous to eqn (41) directly from

$$\Delta\tilde{\Pi}_d = \frac{\phi_+(T/2) + \phi_-(T/2) - 2\phi_s}{2\phi_s}, \quad (46)$$

where ϕ_+ and ϕ_- are the total volume fractions of positive and negative ions (including background salt), respectively, and where ϕ_s is the volume fraction of inert salt in the reservoir.

4 Results and discussion

In this section, we will first discuss the analytical results, followed by a comparison with SCF computations.

4.1 Analytical results

When two charged amphoteric plates in an electrolyte solution are brought to inter-plate separations $h \lesssim \lambda_D$, the electric field between the plates should be sufficiently small for the zero-field treatment of the preceding sections to apply. In the limit of two touching plates, we find a finite contact Donnan potential due to a complete discharging of the plates. This behavior can be clearly seen in Fig. 2: there is no divergence of the potential $\psi = uk_B T/e$ for small h/λ . Since the disjoining pressure $\Delta\tilde{\Pi}_d$ is directly determined by the Donnan potential, the disjoining pressure at contact also remains finite. Remarkably, the contact potential u_0 (eqn (25)) is fully determined by the equilibrium constants pK_1 and pK_2 and the salt concentration; it is therefore independent of the density σ_{tot} of amphoteric surface groups.

Fig. 2 also shows various approximations to the zero-field theory for the parameters listed in Table 1 (first section, $pK_1 = 1$). For two amphoteric plates at pH 6 (1 pH unit from the IEP), we observe large potentials for small separations. Consequently, the low-potential approximations (dashed blue curves) for the electric potential and pressure are not valid in such cases. However, upon increasing the separation, the electric potential gradually decreases and the low-potential approximation becomes valid,

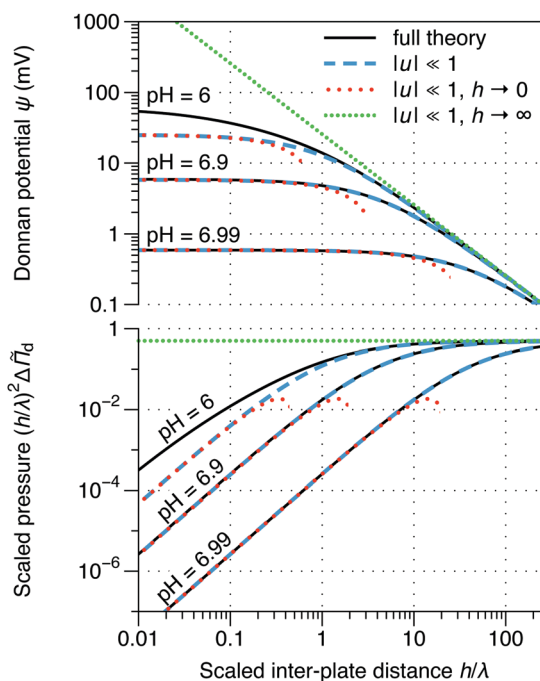


Fig. 2 Comparison of various approximations for the Donnan potential $\psi = uk_B T/e$ and disjoining pressure $\Delta\tilde{\Pi}_d$ for two parallel plates grafted with amphoteric groups ($\sigma_{\text{tot}} = 1 \text{ nm}^{-2}$) according to the zero-field Donnan theory. Equations plotted (top to bottom in legend): (potential) eqn (19), (26), (29) and (31); (pressure) eqn (42)–(45). The dissociation constants are $pK_1 = 1$ and $pK_2 = 13$ (IEP at pH 7) and the total ionic strength is held constant at $I = 10^{-6}$ M ($\lambda_D = 304$ nm). More details on the parameters can be found in Table 1.

Table 1 Overview of relevant parameters for zero-field theory and SCF computations shown in Fig. 2–5. The contact potential and effective contact potential are displayed here as $\psi_0 = u_0 k_B T / e$ and $\psi_0^{\text{eff}} = u_0^{\text{eff}} k_B T / e$, respectively. Note that the presence of additional inert background salt in the zero-field theory is implicitly accounted for through a shift in the pK 's and pH; the reported σ values for k_1 and k_2 include this shift. For all systems, $\sigma_{\text{tot}} = 1 \text{ nm}^{-2}$. Identical values are not repeated

pK_1	pK_2	pH	I (M)	λ_D (nm)	λ (nm)	ψ_0 (mV)	ψ_0^{eff} (mV)	λ/u_0^{eff} (nm)	k_1	k_2	α_+^{max}	α_-^{max}
1	13	6	10^{-6}	304	1.64×10^1	59.1	25.2	1.7×10^1	1.0×10^5	1.0×10^{-7}	1.0×10^{-5}	1.0×10^{-7}
		6.5			4.73	29.6	21.0	5.8	3.2×10^5	3.2×10^{-7}	3.2×10^{-6}	3.2×10^{-7}
		6.9			7.71×10^{-1}	5.91	5.81	3.4	7.9×10^5	7.9×10^{-7}	1.3×10^{-6}	7.9×10^{-7}
		6.99			7.65×10^{-2}	0.591	0.591	3.3	9.8×10^5	9.8×10^{-7}	1.0×10^{-6}	9.8×10^{-7}
3	10	4	10^{-4}	30.4	1.51×10^3	148	28.2	1.4×10^3	1.0×10^1	1.0×10^{-6}	9.1×10^{-2}	9.1×10^{-7}
		7			1.49×10^3	59.1	27.6	1.4×10^3	1.0×10^{-3}	9.1×10^{-2}	9.1×10^{-4}	
		6			1.35×10^3	29.6	22.5	1.5×10^3	1.0×10^{-2}	9.0×10^{-2}	9.0×10^{-3}	
		5.5			1.00×10^3	14.8	13.8	1.9×10^3	3.2×10^{-2}	8.8×10^{-2}	2.8×10^{-2}	
-1	15	6.5	10^{-6}	304	4.73×10^{-2}	29.6	21.0	5.8×10^{-2}	3.2×10^7	3.2×10^{-9}	3.2×10^{-8}	3.2×10^{-9}

even though the contact potential is large. For pH 6.9 and 6.99, closer to the IEP, the low potential approximation is valid over the entire range.

Within the low potential approximation, the contact potential u_0^{eff} dictates the decay of the electric potential and disjoining pressure with the scaled distance h/λ . The initial decay is linear, with a slope set by u_0^{eff} , see eqn (29) and (44) (red dotted curve). This contrasts surfaces with a constant charge or a single dissociation equilibrium, which feature a divergence of the disjoining pressure with h^{-1} and $h^{-1/2}$, respectively, in the limit of small separations.¹⁹ This is the so-called Van 't Hoff regime, where the repulsion is dominated by an 'ideal gas' of counterions. The full discharging of amphoteric surfaces at contact (eqn (35)) prevents this divergence.

However, at large separations the decay becomes independent of u_0^{eff} , see eqn (31) and (45) (green dotted curve). When scaling the disjoining pressure as $(h/\lambda)^2 \Delta \tilde{\Pi}$, this universal inverse square decay displays as a horizontal plateau. It is evident however that, closer to the IEP an increasingly large separation h/λ is required to reach this limit. This is connected to the small contact potential u_0^{eff} , see Table 1, because the large-separation limit only holds for $h \gg \lambda/u_0^{\text{eff}}$.

This brings us to the question: under which conditions can the inverse square decay occur in practical amphoteric systems? First of all, we note that the zero-field approximation is only valid within the unscreened regime, *i.e.*, for strongly overlapping double layers or $h \lesssim \lambda_D$. Second, the electric potential must be small, which is generally true for $h \gg \lambda$ even in case of large contact Donnan potentials. (Naturally, for small contact potentials, this condition is met regardless of separation.) Finally, to access the inverse square decay of eqn (45), the condition $h \gg \lambda/u_0^{\text{eff}}$ must be met. This suggests that, depending on the value of λ , it may become impossible to access the inverse square decay for increasingly small contact potentials, since the Debye screening may come into effect first. However, the values in Table 1 do suggest that at least under certain combinations of parameters the inverse square decay could be observable.

4.2 Comparison to SCF

To investigate the validity and accuracy of our zero-field theory for two amphoteric surfaces, we will now compare the results

to self-consistent field (SCF) computations that solve the full Poisson–Boltzmann equation and in which ions have a finite size.

First we devote our attention to the situation at large Debye length, when the ionic strength is low ($I = 10^{-6}$ M, $\lambda_D = 0.3 \mu\text{m}$), see Fig. 3. For these systems, we set a large difference between the two equilibrium constants ($pK_1 = 1$, $pK_2 = 13$) and the pH is rather close to the IEP, entailing very small degrees of dissociation. A full overview of all parameters is given in the first section of Table 1 ($pK_1 = 1$).

From Fig. 3 it is evident that the zero-field Donnan treatment gives a quantitative prediction of the electric potential, the net degree of dissociation, and the disjoining pressure for the parameters in question. We can identify three distinct regimes in Fig. 3:

1. Relatively far from the IEP (*e.g.*, a pH of 6), the electric potential is large for small h . In this regime, the decay of u and $\Delta \tilde{\Pi}_d$ is governed by λ .

2. For intermediate separations, $h \gtrsim \lambda$, the system enters the low-potential limit, and the length scale of the decay is set by λ/u_0^{eff} following eqn (26) and (43).

3. Finally, for large separations, the decay is once again set by λ , however the decay is now universal: the absolute value of potential and pressure becomes independent of the contact potential, following eqn (31) and (45).

Close to the IEP (pH 6.9 and 6.99), the contact potentials are small: regime (1) is not present and regime (2) holds until the plates touch. Additionally, all curves appear to be similar, except for a different pre-factor. This is because close to the IEP, where $k_1 k_2 \approx 1$, the factor λ/u_0^{eff} becomes constant:

$$\frac{\lambda}{u_0^{\text{eff}}} \simeq \frac{\sigma_{\text{tot}}}{\rho_s} \frac{2}{2 + k_1} \quad \text{for } k_1 k_2 \approx 1. \quad (47)$$

This can also be verified numerically from the data in Table 1. Thus, in the vicinity of the IEP, a particular system will have a universal behavior regardless of the precise distance to the IEP, differing only by a pre-factor set by u_0^{eff} .

We now turn our attention to the situation an ionic strength of $I = 10^{-4}$ M ($\lambda_D = 30$ nm), see Fig. 4. The systems shown here have a fixed pH of 7 and $pK_1 = 3$. The second equilibrium

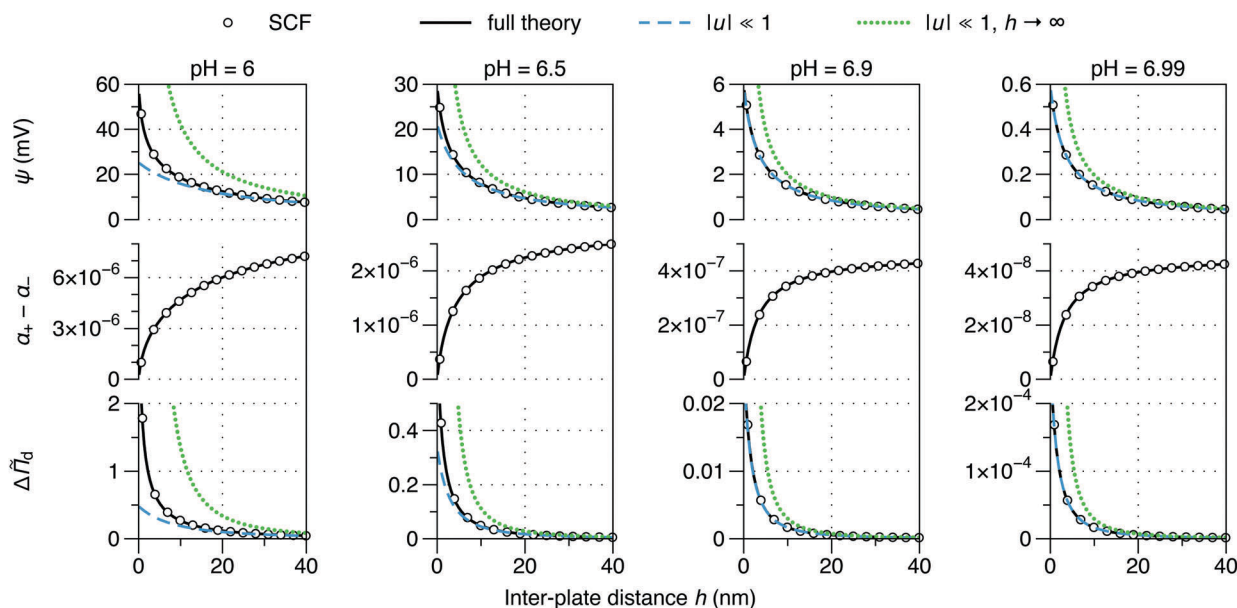


Fig. 3 Comparison between zero-field theory (solid black curve) and SCF computations (open circles) for the Donnan potential $\psi = uk_B T/e$, net degree of dissociation $\alpha_+ - \alpha_-$, and disjoining pressure $\Delta\bar{\Pi}_d$ for two parallel plates grafted with amphoteric groups ($\sigma_{\text{tot}} = 1 \text{ nm}^{-2}$) as a function of the inter-plate distance h at the indicated pH values. The dissociation constants are $pK_1 = 1$ and $pK_2 = 13$ (IEP at pH 7) and the total ionic strength is held constant at $I = 10^{-6} \text{ M}$ through additional inert background salt ($\lambda_D = 304 \text{ nm}$). More details on the parameters can be found in Table 1. Equations of zero-field theory plotted (left to right in legend): (potential) eqn (19), (26) and (31); (dissociation) eqn (34); (pressure) eqn (42), (43) and (45).

constant pK_2 is varied, but in general pK_1 and pK_2 are significantly closer together than in the previous example. A detailed overview of all parameters is shown in the second section of Table 1 ($pK_1 = 3$).

From Fig. 4 it is immediately apparent that beyond separations comparable to the Debye length, the zero-field assumption starts to

break down: screening comes into effect and the predicted potential, degree of dissociation, and disjoining pressure as predicted by the Donnan model are all higher than the numerical SCF results. At small separations $h \lesssim 15 \text{ nm}$ the zero-field approach is still valid. However, because Debye screening occurs at larger separations, the low potential limit cannot be realized in these systems.

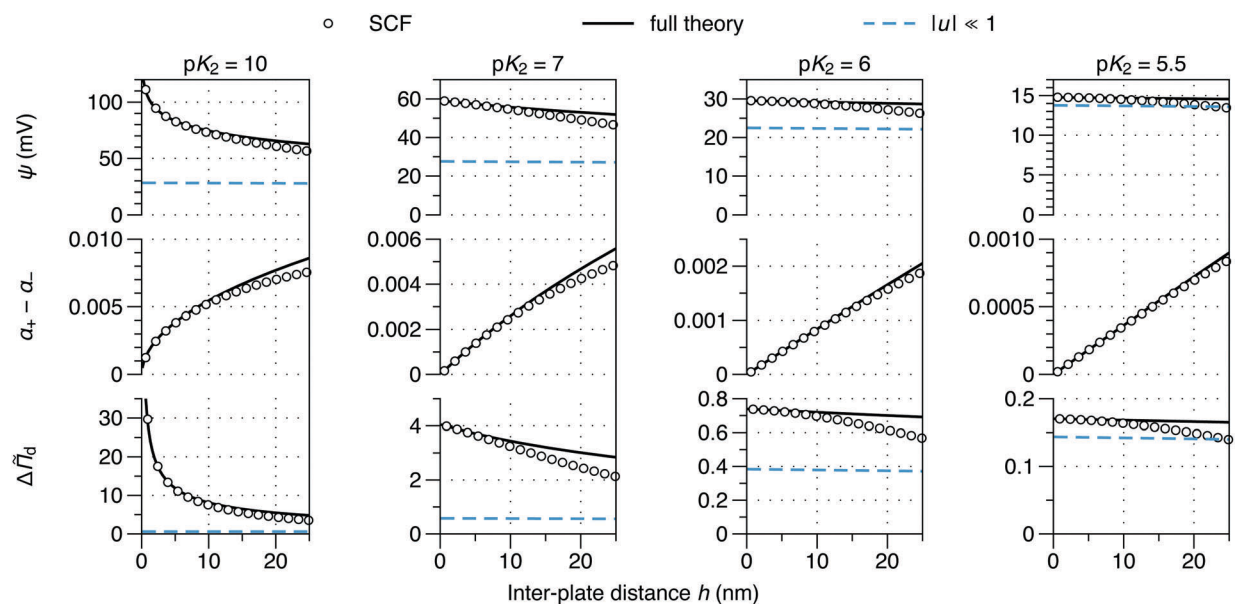


Fig. 4 Comparison between zero-field theory and SCF computations for the Donnan potential $\psi = uk_B T/e$, net degree of dissociation $\alpha_+ - \alpha_-$, and disjoining pressure $\Delta\bar{\Pi}_d$ for two parallel plates grafted with amphoteric groups ($\sigma_{\text{tot}} = 1 \text{ nm}^{-2}$) as a function of the inter-plate distance h . The dissociation constant $pK_1 = 3$ and pK_2 is varied as indicated. The pH is 4 with no additional inert salt (ionic strength $I = 10^{-4} \text{ M}$, $\lambda_D = 30.4 \text{ nm}$). More details on the parameters can be found in Table 1. Equations of zero-field theory plotted (left to right in legend): (potential) eqn (19) and (26); (dissociation) eqn (34); (pressure) eqn (42) and (43).

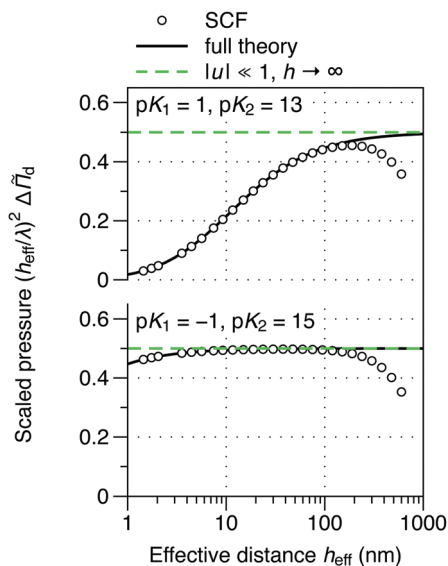


Fig. 5 Manifestation of inverse square decay of disjoining pressure with separation h_{eff} of two amphoteric plates. The dissociation constants are (top) $pK_1 = 1$ and $pK_2 = 13$, and (bottom) $pK_1 = -1$ and $pK_2 = 15$ (IEP at pH 7). The ionic strength is $I = 10^{-6}$ M through additional inert background salt ($\lambda_D = 304$ nm) and the pH is 6.5. The pressure is scaled as $(h_{\text{eff}}/\lambda)^2 \Delta \tilde{\Pi}_d$, such that the inverse square decay appears as a horizontal plateau. The effective inter-plate distance h_{eff} is defined in eqn (48). From the zero-field theory eqn (42) (full theory) and eqn (45) ($|u| \ll 1, h \rightarrow \infty$) are shown.

There are also qualitative differences between the systems currently at hand and those previously discussed in Fig. 3. The systems in Fig. 4 feature a very long-ranged decay of potential and disjoining pressure with distance. The reason is that the length scale λ for these systems is very large, of the order of 1 μm . As can be seen from eqn (20a), this is because there is a large net degree of dissociation, as one of the pK 's is rather close to the pH.

Additionally, for $pK_2 = 10$ there is a characteristic (rather sharp) upturn of $\psi = uk_B T/e$ and $\Delta \tilde{\Pi}_d$ at small h , which precedes the slow decay of potential and pressure. This upturn is related to the fact that surfaces with a single dissociation equilibrium have an infinite contact potential. Here, the second dissociation equilibrium is very weak compared to the first equilibrium, such that it is practically absent. The divergence of the contact electric potential and contact disjoining pressure thus slowly reappears when one of the equilibria becomes negligible.

Finally, we turn our attention to the inverse square decay of pressure with separation. Since the focus of the current work is on amphoteric surfaces, we will restrict ourselves to systems close to the IEP, such that both equilibria play a role. As discussed in the previous section, the observation of this behavior is most likely when simultaneously the Debye length is relatively large and both λ and λ/u_0^{eff} are small. The latter can be judged from eqn (47). For systems close to the IEP, it turns out that λ/u_0^{eff} is small when k_1 is large. Because close to the IEP $k_1 k_2 \approx 1$, this means that k_2 must be small. In other words, there should be a large difference between pK_1 and pK_2 .

This requirement is illustrated in Fig. 5, which shows two systems with (top) $\Delta pK = pK_2 - pK_1 = 12$ (same as in Fig. 3, pH 6.5)

and (bottom) $\Delta pK = 16$ (see also Table 1, third section, $pK_1 = -1$). The pressure is scaled as $(h/\lambda)^2 \Delta \tilde{\Pi}_d$, and the effective inter-plate distance

$$h_{\text{eff}} = h - 2\sigma_{\text{tot}} b^3 \quad (48)$$

takes into account the finite volume of the surface groups.¹⁴ It is evident that in the first case the plateau value $(h/\lambda)^2 \Delta \tilde{\Pi}_d = 0.5$, characteristic for the inverse square decay, is not fully developed due to the occurrence of Debye screening at $h \approx 10^2$ nm. Increasing ΔpK to 16 decreases λ hundredfold, while keeping u_0^{eff} constant, see Table 1. This indeed makes the inverse square decay clearly apparent.

It should be stressed that our SCF computations incorporate a treatment of Poisson–Boltzmann theory on a mean-field level. Therefore, deviations from Poisson–Boltzmann theory (such as due to overcharging²⁹ or under confinement³⁰) are not accounted for. We leave further discussion on the general validity of Poisson–Boltzmann theory for other work; we note here that our results show that the zero-field Donnan model represents an insightful treatment of repulsions between amphoteric plates with strongly overlapping double layers on the level of Poisson–Boltzmann theory.

5 Conclusions

The entropic repulsion between two amphoteric surfaces has been analyzed in the limit of zero electric field, where ideal ions are homogeneously distributed in the inter-plate solution and are in equilibrium with a reservoir with constant salt concentration. We show that there is an inherent length scale λ that governs the decay of electric potential and disjoining pressure with inter-plate distance, which serves as the unscreened counterpart of the Debye length. In the limit of low potentials, we show that the decay is set by an effective contact potential u_0^{eff} and the length scale λ . Further, the zero-field disjoining pressure between amphoteric surfaces has an inverse-square decay for low potentials and sufficient inter-plate distances, just as for constant-charge surfaces and surfaces with a single dissociation equilibrium, be it with a smaller amplitude due to the charge regulation. This is remarkable, because in general scaling depends on the precise boundary conditions (*i.e.*, constant charge, constant potential, or charge regulation). Numerical self-consistent field lattice computations quantitatively confirm the predictions of the zero-field model, including the inverse square decay for large separations and small potentials. Additionally, the zero-field model remains valid at large electric potentials, showing that Donnan theory is a tractable way to describe repulsions between amphoteric charged plates separated by distances smaller than the Debye length. The results described here have direct practical relevance, for instance to understand electrostatic interactions in self-assembled multi-layered structures, such as microtubes or membranes. A pertinent continuation for future work would be an extension of the present model towards non-flat geometries, such as concentrated dispersions of amphoteric colloids with average particle separations of the order of the Debye length.

Conflicts of interest

There are no conflicts to declare.

Acknowledgements

M. V. and R. T. would like to thank Prof. Frans Leermakers for providing the SFbox software package. M. V. acknowledges the Netherlands Organisation for Scientific Research (NWO) for a Veni grant (no. 722.017.005). The authors would like to thank Landman *et al.*¹⁶ for sharing a preprint of their manuscript.

References

- 1 E. J. W. Verwey and J. T. G. Overbeek, *Theory of the stability of lyophobic colloids*, Dover Publications, 1999.
- 2 B. Chu and P. J. W. Debye, *Molecular forces: Based on the Baker lectures of Peter J. W. Debye*, Interscience Publishers, 1967.
- 3 J. T. G. Overbeek, *Colloid science*, Elsevier, Amsterdam, 1952, vol. 2.
- 4 J. N. Israelachvili, *Intermolecular and surface forces*, Academic Press, 2015.
- 5 T. Cosgrove, *Colloid science: principles, methods and applications*, John Wiley & Sons, 2010.
- 6 K. Dill and S. Bromberg, *Molecular driving forces: statistical thermodynamics in biology, chemistry, physics, and nano-science*, Garland Science, 2010.
- 7 D. F. Evans and H. Wennerström, *The Colloidal Domain*, Wiley-VCH, 1999.
- 8 P. C. Hiemenz and R. Rajagopalan, *Principles of Colloid and Surface Chemistry*, Marcel Dekker, 1997.
- 9 W. B. Russel, D. A. Saville and W. R. Schowalter, *Colloidal dispersions*, Cambridge University Press, 1989.
- 10 T. F. Tadros, *Colloid stability: the role of surface forces*, Wiley-VCH, 2007.
- 11 P. M. Biesheuvel, *J. Colloid Interface Sci.*, 2001, **238**, 362–370.
- 12 T. Markovich, D. Andelman and R. Podgornik, 2016, arxiv:1603.09451.
- 13 A. P. Philipse, B. W. M. Kuipers and A. Vrij, *Langmuir*, 2013, **29**, 2859–2870.
- 14 A. P. Philipse, R. Tuinier, B. W. M. Kuipers, A. Vrij and M. Vis, *Colloid Interface Sci. Commun.*, 2017, **21**, 10–14.
- 15 F. J. M. Ruiz-Cabello, M. Moazzami-Gudarzi, M. Elzbienciak-Wodka, P. Maroni, C. Labbez, M. Borkovec and G. Trefalt, *Soft Matter*, 2015, **11**, 1562–1571.
- 16 J. Landman, S. Ouhajji, S. Prévost, T. Narayanan, J. Groenewold, A. P. Philipse, W. K. Kegel and A. V. Petukhov, *Sci. Adv.*, 2018, DOI: 10.1126/sciadv.aat1817.
- 17 S. Schneider and P. Linse, *J. Phys. Chem. B*, 2003, **107**, 8030–8040.
- 18 S. Schneider, PhD thesis, Lund University, 2003.
- 19 T. Markovich, D. Andelman and R. Podgornik, *EPL*, 2016, **113**, 26004.
- 20 G. J. Fleer, M. A. Cohen Stuart, J. M. H. M. Scheutjens, T. Cosgrove and B. Vincent, *Polymers at interfaces*, Springer Science & Business Media, 1993.
- 21 F. A. M. Leermakers, J. C. Eriksson and J. Lyklema, *Fundamentals of interface and colloid science: soft colloids*, Academic Press, 2005, vol. 5.
- 22 J. van Male, PhD thesis, Wageningen University, 2003.
- 23 J. M. H. M. Scheutjens and G. J. Fleer, *J. Phys. Chem.*, 1979, **83**, 1619–1635.
- 24 M. R. Böhmer, O. A. Evers and J. M. H. M. Scheutjens, *Macromolecules*, 1990, **23**, 2288–2301.
- 25 S. M. Oversteegen and F. A. M. Leermakers, *Phys. Rev. E: Stat. Phys., Plasmas, Fluids, Relat. Interdiscip. Top.*, 2000, **62**, 8453–8461.
- 26 O. A. Evers, J. M. H. M. Scheutjens and G. J. Fleer, *Macromolecules*, 1990, **23**, 5221–5233.
- 27 P. N. Hurter, J. M. H. M. Scheutjens and T. A. Hatton, *Macromolecules*, 1993, **26**, 5592–5601.
- 28 P. J. Flory, *Principles of Polymer Chemistry*, Cornell University Press, Ithaca, NY, 1953.
- 29 M. Quesada-Pérez, E. González-Tovar, A. Martn-Molina, M. Lozada Cassou and R. Hidalgo-Alvarez, *ChemPhysChem*, 2003, **4**, 234–248.
- 30 L. Yeomans, S. E. Feller, E. Sánchez and M. Lozada Cassou, *J. Chem. Phys.*, 1993, **98**, 1436–1450.